Supplementary Information (SI) for Manuscript: *Genetic screening reveals phospholipid metabolism as a key regulator of the biosynthesis of the redox-active lipid coenzyme Q*

Anita Ayer[a,b], Daniel J. Fazakerley[c,d], Cacang Suarna[a,b], Ghassan J. Maghzal[b], Diba Sheipouri[b], Kevin J. Lee[b], Michelle C. Bradley[e], Lucía Fernández-del-Rio[e], Sergey Tumanov[a,b], Stephanie MY Kong[a,b], Jelske N. van der Veen[f], Andrian Yang,[b,g], Joshua W.K. Ho[b,g,h,i], Steven G. Clarke[e], David E. James[c], Ian W. Dawes[j], Dennis E. Vance[k], Catherine F. Clarke[e], René L. Jacobs[f] and Roland Stocker[a,b,g,l]*

Affiliations:

[a]Heart Research Institute, The University of Sydney; Sydney, New South Wales, Australia
[b]Victor Chang Cardiac Research Institute; Sydney, Australia
[c]Charles Perkins Centre, School of Life and Environmental Sciences, Sydney Medical School, The University of Sydney; Sydney, Australia
[d]Metabolic Research Laboratory, Wellcome-Medical Research Council Institute of Metabolic Science, University of Cambridge; Cambridge, United Kingdom
[e]Department of Chemistry and Biochemistry, and the Molecular Biology Institute, University of California; Los Angeles, United States
[f]Department of Agricultural, Food and Nutritional Science, University of Alberta; Edmonton, Canada
[g]St Vincent's Clinical School, University of New South Wales, Sydney, Australia
[h]School of Biomedical Sciences, Li Ka Shing Faculty of Medicine, University of Hong Kong, Hong Kong SAR, China
[i]Laboratory for Data Discovery for Health, Hong Kong Science Park, Hong Kong SAR, China
[j]School of Biotechnology and Biomolecular Sciences, University of New South Wales; Sydney, Australia
[k]Department of Biochemistry, University of Alberta; Edmonton, Canada
[l]School of Life and Environmental Sciences, The University of Sydney, Sydney, Australia

***Corresponding author: Roland Stocker**
Address: Heart Research Institute, 7 Eliza St Newtown, Australia 2042
Email: roland.stocker@hri.org.au

This PDF file includes:

Table S2. Genotype and source of yeast strains

Strain	Genotype	Source
BY4743	*MAT***a**/*MATα his3Δ1/his3Δ1 leu2Δ0/leu2Δ0 LYS2/lys2Δ0 met15Δ0/MET15 ura3Δ0/ura3Δ0*	(1)
Homozygous diploid strains	*MAT***a**/*MATα his3Δ1/his3Δ1 leu2Δ0/leu2Δ0 LYS2/lys2Δ0 met15Δ0/MET15 ura3Δ0/ura3Δ0 Gene of interest::KanMX*	(2)
BY4743 *CHO2* heterozygous	*MATα his3Δ1 leu2Δ0 lys2Δ0 ura3Δ0; MATa his3Δ1 leu2Δ0 met15Δ0 ura3Δ0 CHO2::KanMX*	This study
BY4743 rho^0	*MAT***a**/*MATα his3Δ1/his3Δ1 leu2Δ0/leu2Δ0 LYS2/lys2Δ0 met15Δ0/MET15 ura3Δ0/ura3Δ0; respiratory incompetent*	This study
BY4742	*MATα his3Δ1 leu2Δ0 lys2Δ0 ura3Δ0*	
BY4741	*MAT**a** his3Δ1 leu2Δ0 met15Δ0 ura3Δ0*	R. Yang
BY4741 *cho2Δ*	*MAT**a** his3Δ1 leu2Δ0 met15Δ0 ura3Δ0 CHO2::KanMX*	R. Yang
BY4741 *ste14Δ*	*MAT**a** his3Δ1 leu2Δ0 met15Δ0 ura3Δ0 STE14::KanMX*	R. Yang
BY4742 *coq1*Δ	*MATα his3Δ0 leu2Δ0 met15Δ0 ura3Δ0 COQ1::KanMX4*	(2)
BY4742 *coq3*Δ	*MATα his3Δ0 leu2Δ0 met15Δ0 ura3Δ0 COQ 3::KanMX4*	(2)
BY4742 *coq4*Δ	*MATα his3Δ0 leu2Δ0 met15Δ0 ura3Δ0 COQ 4::KanMX4*	(2)
BY4742 *coq5*Δ	*MATα his3Δ0 leu2Δ0 met15Δ0 ura3Δ0 COQ 5:: KanMX4*	(2)
BY4741*coq6*Δ	*MATα his3Δ0 leu2Δ0 met15Δ0 ura3Δ0 COQ 6::KanMX4*	(2)
BY4742 *coq7*Δ	*MATα his3Δ0 leu2Δ0 met15Δ0 ura3Δ0 COQ 7::KanMX4*	(2)
BY4742 *coq8*Δ	*MATα his3Δ0 leu2Δ0 met15Δ0 ura3Δ0 COQ::KanMX4*	(2)
BY4742 *coq9*Δ	*MATα his3Δ0 leu2Δ0 met15Δ0 ura3Δ0 COQ9::KanMX4*	(2)
BY4742 *coq10*Δ	*MATα his3Δ0 leu2Δ0 met15Δ0 ura3Δ0 COQ10::KanMX4*	(2)
BY4742 *coq11*Δ	*MATα his3Δ0 leu2Δ0 met15Δ0 ura3Δ0 coq11::LEU2*	(3)
W303-1a	*MATa leu2-3,112 trp1-1 can1-100 ura3-1 ade2-1 his3-11,15*	A. Cooper
W303-1a *cho2Δ*	*MAT**a** leu2-3,112 trp1-1 can1-100 ura3-1 ade2-1 his3-11,15 CHO2::NatMX*	This study

Table S3. Primers used in this study

Name	Primer sequence (5'-3')	Source
CHO2-S1	TTTCGAGTGATTTTCTTAGTGACAAAGC TTTTTCTTCATCTGTAGATGCGTACGCTG CAGGTCGAC	This study
CHO2-S2	GAATCCTAGTACTTTTTAAATATATATA CTCAAAAAAAAAAAACTCAATCGATGA ATTCGAGCTCG	This study
CHO2-A	ATACAGATTCTTTCCACTGTGTTCC	(4)
CHO2-D	GCTGTTTAATGAACCAGGAAACTTA	(4)
CHO2-F	GTGATATTATTGACACGCCCATGTCCAG TTGTAAAACC	This study
CHO2-R	GGGATCACCATCCGTCGCCCTCAAGCAA GACTATCAAG	This study
mtDNA F	GTGCGTATATTTCGTTGATGCGT	(5)
mtDNA R	TTCACACTGCCTGTGCTATCTAA	(5)
yACT1F	TATGTTCTAGCGCTTGCACCA	This study
yACT1R	CCAAAGCAGCAACCTCTAAA	This study
yCOQ1F	CCCGAAGTCGTAGAACTAATG	This study
yCOQ1R	GGAACCGGAAGTAGCTTATG	This study
yCOQ2F	CAGCTGGTATGTTGGGTATTT	This study
yCOQ2R	GACGGACCTGATAACTCTTTG	This study
yCOQ3F	CATGCTGGAGGGAAAGATAAA	This study
yCOQ3R	TCGACCAACAATGCCTTAAA	This study
yCOQ4F	GTGGTATCCTTGCACCTTTAC	This study
yCOQ4R	CCAGCATTTCCTCCCAATAC	This study
yCOQ5F	TGCTTAAAGAAGGTGAGAAGAG	This study
yCOQ5R	TACCGAAGGAGACTGTGTAG	This study
yCOQ6F	TGAAGGACGAGTCGGATATT	This study
yCOQ6R	CCAACAAGGGCAACTCTATC	This study
yCOQ7F	GCTCCCAAGTGTCAGAATTTA	This study
yCOQ7R	CTGGTCCCATATGTGCTTTAG	This study
yCOQ8F	CGTATGGAGGGAACTGAAATAA	This study
yCOQ8R	GAGGCACCGAAATCCAATAA	This study
yCOQ9F	CGCTGTCATGGAACTGATAAA	This study
yCOQ9R	GAGAAAGGCGCTTGGAATAG	This study
yCOQ10F	GCGGTACCAATCACACTATTA	This study
yCOQ10R	GAGAGGCTTGTTATCCACAG	This study
yCOQ11F	GCAGAGATATTTCAGGCCTATTA	This study
yCOQ11R	CTGCTGAGTGGATACTGTTG	This study
mPDSS1F	ACACCAGCAATGTGCAGTTG	This study
mPDSS1R	ACAGACCTTTCAAGTCTCTCCAG	This study
mPDSS2F	CGCTTGTCCGGTTACCTCG	This study
mPDSS2R	GGGTAGCCCACGATCTTCTC	This study
mCOQ2F	ACAAGCCCATAGGAACCTGG	This study
mCOQ2R	CTCCACGCATCAGAATAGCTC	This study
mCOQ3F	CTCGTGGGGTTCGTCTCCT	This study
mCOQ3R	GAGCTGCGTCCCTGAGTAAG	This study
mCOQ4F	TGTACCCGGACCACATCCC	This study
mCOQ4R	AACCATGTCGTGGCGATAGG	This study
mCOQ5F	CCCAGGTGCTGCGTTCTATG	This study
mCOQ5R	GTCTCAAACCCGAAGTGCG	This study
mCOQ6F	CTCAGCAGTTTTGGTGCATGG	This study

mCOQ6R	TGTCCCTGTCGAACATTATCAAG	This study
mCOQ7F	ACGAGTTGATGATTGCATTCAGG	This study
mCOQ7R	TTCCCCAGCAAGGCAGTTC	This study
mCOQ8F	CCATTGGGCAGGTACACCAAG	This study
mCOQ8R	CTCTGCGGTAGTCACATTCCC	This study
mCOQ9F	GTGGGGTTCCGGTCTTCAG	This study
mCOQ9R	GGGGTGGACGGGAAAACTC	This study
mCOQ10F	CAGCTCGGACCAGTCAGAG	This study
mCOQ10R	TCCTCCATTCCTGATACTACGTC	This study
mβACTF	GGATGCAGAAGGAGATCACTG	(6)
mβACTR	CGATCCACACGGAGTACTTG	(6)
mCYCBF	TTCTTCATAACCACAGTCAAGACC	(7)
mCYCBR	ACCTTCCGTACCACATCCAT	(7)
mPEMTF	TGGCTGCTGGGTTACATGG	This study
mPEMTR	GCTTCCGAGTTCTCTGCTCC	This study

Table S4 –Antibody list

Antibody	*Working dilution*	*Source*
Coq1	1:10,000	(8)
Coq2	1:1,000	(9)
Coq3	1:200	(10)
Coq4	1:2,000	(11)
Coq5	1:5,000	(12)
Coq6	1:200	(13)
Coq7	1:1,000	(14)
Coq8	Affinity purified, 1:30	(15)
Coq9	1:1,000	(15)
Coq10	Affinity purified, 1:400	(16)
Coq11	1:500	(16)
Mdh1	1:10,000	Lee McAlister-Henn[a]
Porin (459500)	1:1000	Thermo Fisher Scientific
Tubulin (MAB1501)	1:1000	MP Biomedicals

[a]Dr. Lee McAlister-Henn, Department of Molecular Biophysics and Biochemistry, University of Texas Health Sciences Center, San Antonio, TX

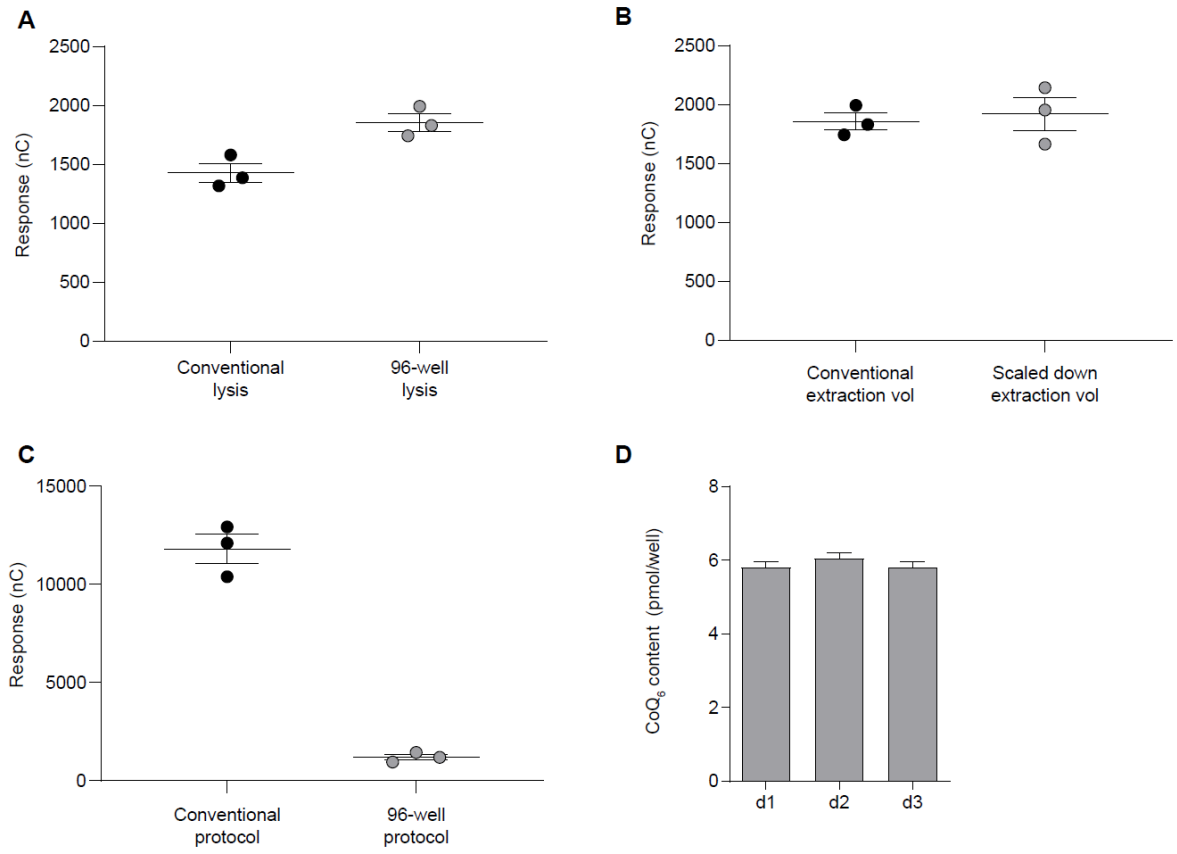

Fig. S1. Development and validation of a 96-well plate method for cell growth, lysis and CoQ extraction of yeast cells. (A) HPLC-ECD analyses of CoQ content in cells lysed either using the conventional process (fast prep) or in a 96-well plate. **(B)** HPLC-ECD analyses of CoQ content in cells extracted either using the conventional volumes of hexane/methanol (12 mL) or scaled down reagent volumes (2.5 mL). **(C)** Comparison of HPLC-ECD response from cells grown, lysed and extracted in the conventional manner versus cells grown, lysed and extracted in a 96-well plate. **(D)** Inter- and intraday reproducibility of cells grown, lysed and extracted in a 96-well plate. Data and error bars depict mean ± s.e.m.

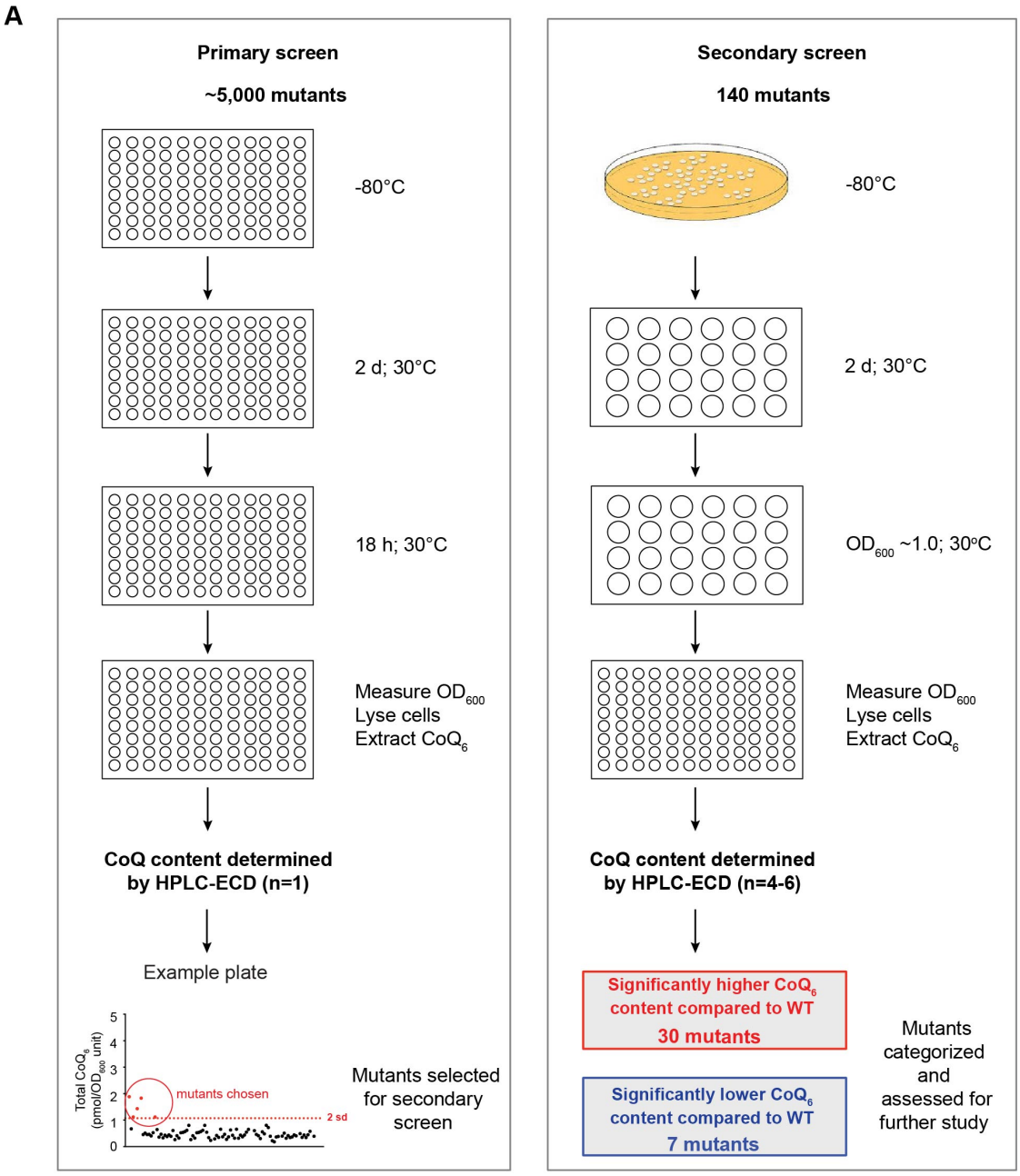

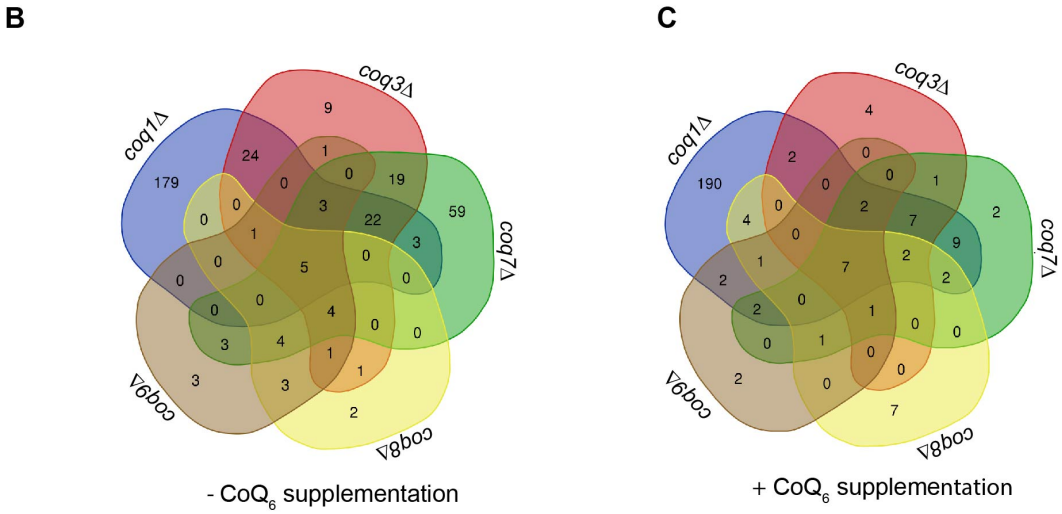

Fig. S2. Schematic representation of the experimental workflow of genetic screen and microarray results. (**A**) *Primary screen:* Frozen stocks of the homozygous diploid yeast knockout collection were thawed, replica plated into 96-well plates containing synthetic defined media lacking CoQ head group

precursors (SD minus 4HB-pABA) and grown for 2 d at 30 °C. Cells were replica plated into fresh SD minus 4HB-pABA in 96-well plates, grown for 18 h at 30 °C and OD_{600} measured before lysis and CoQ_6 extracted. CoQ_6 in each mutant was determined by HPLC-ECD, normalized to biomass and the average CoQ_6 content of mutants on each plate calculated. Mutants with CoQ_6 content two standard deviations above or below the plate population mean were selected for secondary screening. *Secondary screen:* WT BY4743 and selected mutants were recovered from -80 °C glycerol stocks, grown on YEPD agar plates for 2 d at 30 °C, and inoculated into 24-well plates containing SD minus 4HB-pABA for 2 d at 30 °C. Cells were subsequently inoculated into 24-well plates containing SD minus 4HB-pABA and grown at 30 °C to exponential phase ($OD_{600\ nm}$ ~1.0). Cells were lysed, CoQ_6 content in each mutant determined by HPLC-ECD and normalized to biomass. Mutants with significantly higher or lower CoQ_6 content compared to WT were identified for further study. **B-C**) Venn diagram of differentially expressed genes in different *coq* mutants grown in the absence (**B**) or presence (**C**) of CoQ_6 supplementation Abbreviations: 4-HB, 4-hydroxybenzoic acid; CoQ, coenzyme Q; HPLC-ECD, high-performance liquid chromatography-electrochemical detection; OD_{600}, optical density at 600 nm; pABA, *para*-aminobenzoic acid; YEPD, yeast extract peptone dextrose.

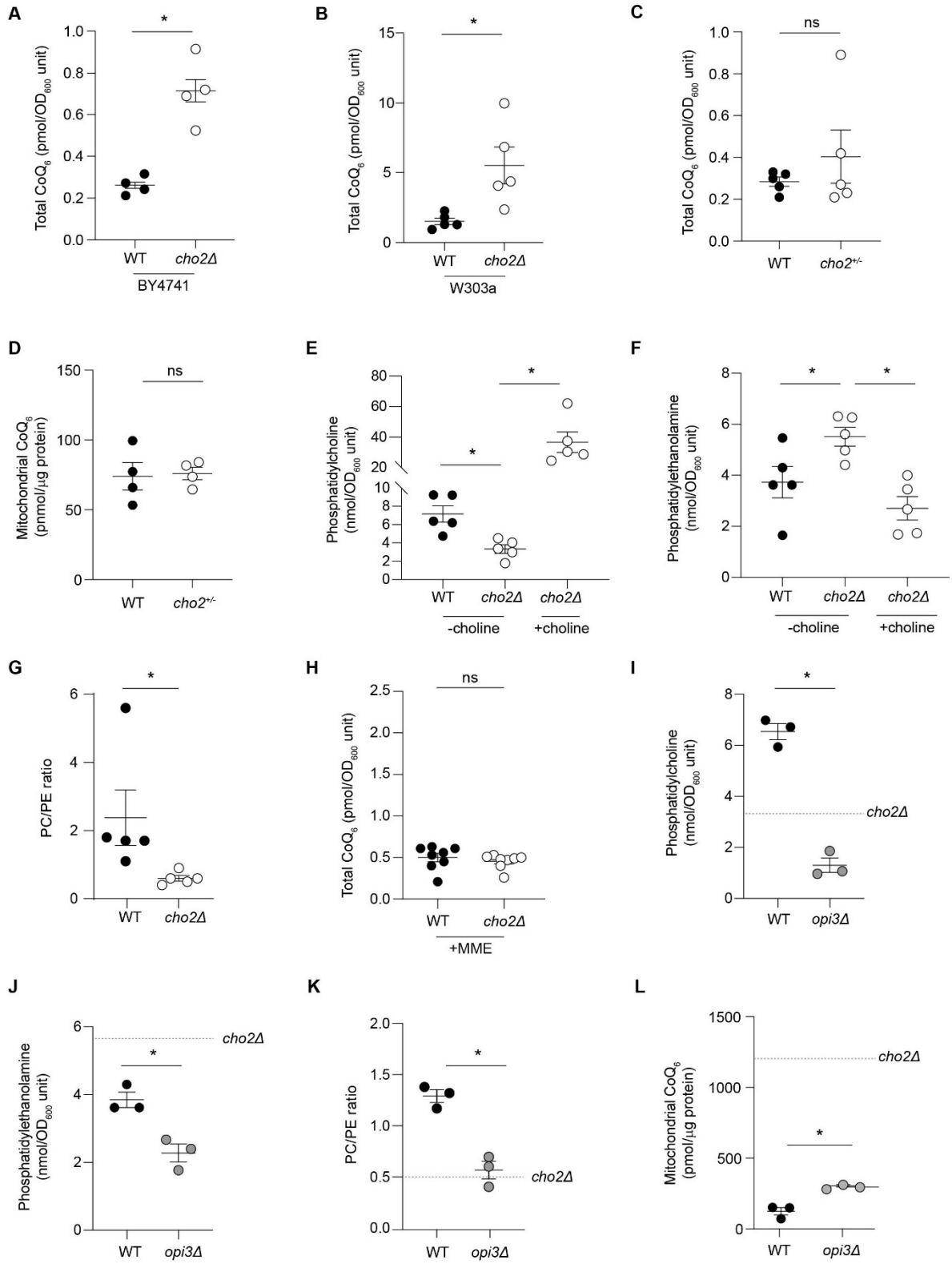

Fig. S3. Deletion of the *CHO2* gene results in increased cellular CoQ_6 content that is independent of phosphatidylcholine concentrations in *S. cerevisiae*. **(A)** Concentration of CoQ_6 in haploid WT and *CHO2* deficient mutants in the BY4741 genetic background (n=4). **(B)** Concentration of CoQ_6 in haploid WT and *CHO2*-deficient mutants in the W303a genetic background (n=5). **(C)** Total CoQ_6 content in WT and yeast cells heterozygous for *CHO2* in the BY4743 background (n=5). **(D)** Mitochondrial CoQ_6 content in WT and yeast cells heterozygous for *CHO2* in the BY4743 background (n=4). **(E)** Phosphatidylcholine concentrations in WT and *cho2Δ* mutants with and without 1 mM choline supplementation (n=5). **(F)** Phosphatidylethanolamine concentrations in WT and *cho2Δ* mutants with and without 1 mM choline supplementation (n=5). **(G)** PC/PE ratio in WT and *cho2Δ* mutants (n=5). **(H)** CoQ_6 concentrations in WT and *cho2Δ* mutants with and without 1 mM monomethylethanolamine (MME) supplementation (n=8). (I) Phosphatidylcholine concentrations in

WT and *opi3Δ* mutants (n=3). **(J)** Phosphatidylethanolamine concentrations in WT and *opi3Δ* mutants (n=3). **(K)** PC/PE in ratio in WT and *opi3Δ* mutants (n=3). **(L)** Mitochondrial CoQ_6 content in WT cells and *opi3Δ* mutants (n=3). For panels **I-L**, dashed lined represents the mean value observed in *cho2Δ* mutants. Data and error bars depict mean ± s.e.m. *P ≤ 0.05 and ns indicates 'not significant' as determined by Mann-Whitney test.

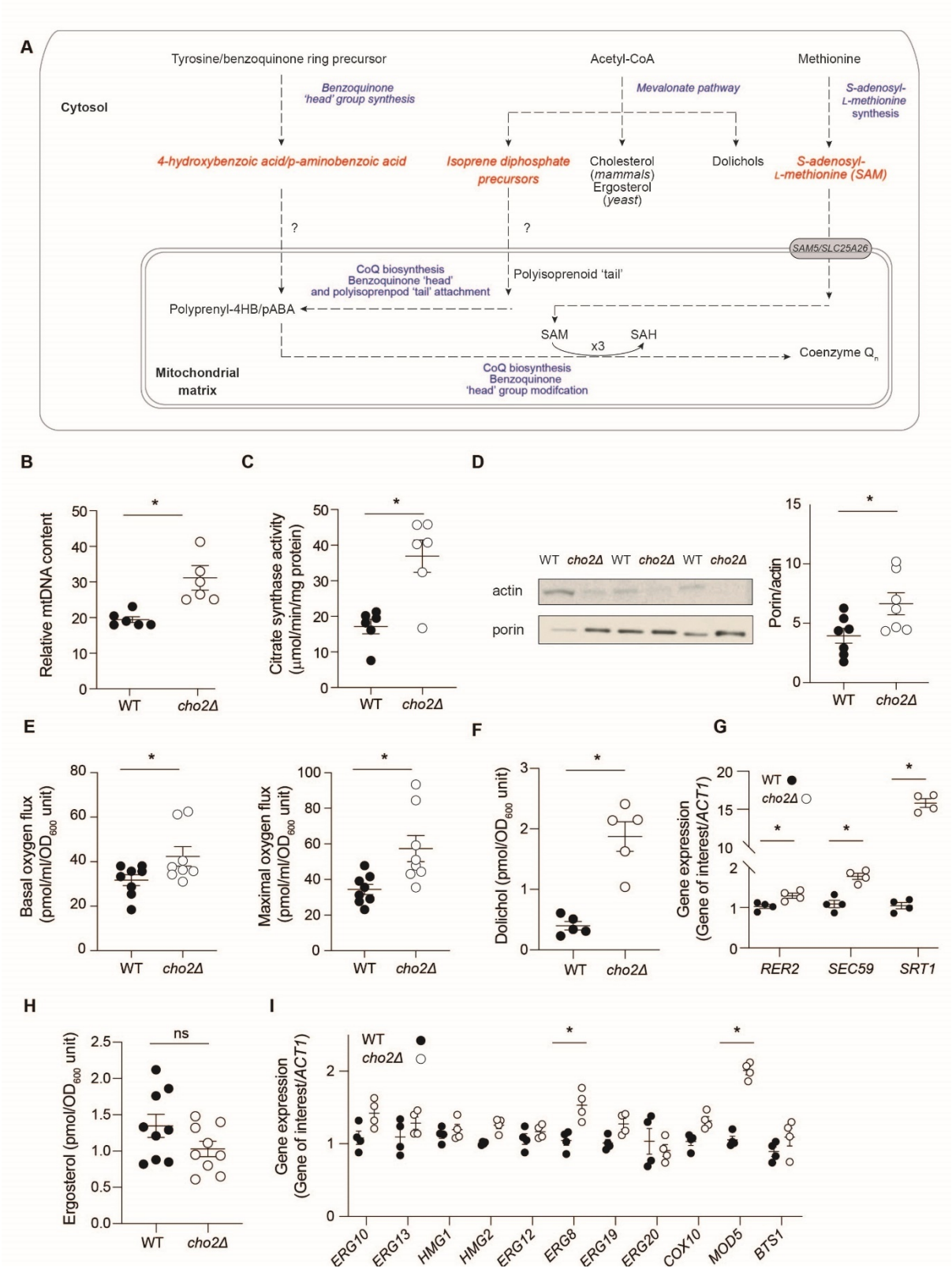

Fig. S4. Increased CoQ_6 in *cho2Δ* cannot be explained by changes in mitochondrial mass or changes in the mevalonate pathway in *S. cerevisiae*. (**A**) Schematic outlining the biochemical pathways involved in CoQ biosynthesis and their cellular localization. Question marks indicate pathways currently not elucidated. (**B-D**) *cho2Δ* mutant have increased mitochondrial mass compared with WT cells (n=6-7) as indicated by increased: mitochondrial DNA content determined by quantitative PCR (**B**), citrate synthase activity (**C**) and porin content determined by Western blotting (**D**). (**E**) Basal and maximal respiration rates in WT and *cho2Δ* mutants as measured by high-resolution respirometry (n=8). (**F**) Dolichol concentration in WT and *cho2Δ* mutants as measured by LC/MS/MS (n=5). (**G**) Gene expression of dolichol synthesis pathway in *cho2Δ* mutants compared to WT determined by qPCR (n=4). (**H**) Ergosterol concentration in WT and *cho2Δ* mutants as measured by

HPLC-UV (n=9). (**I**) Mevalonate pathway gene expression in *cho2Δ* mutants compared to WT determined by qPCR (n=4). Data and error bars depict mean ± s.e.m. *$P \leq 0.05$ and ns indicates 'not significant' as determined by Mann-Whitney test (**B-F, H**) or by 2-way ANOVA with Sidak's multiple comparison test (**G, I**).

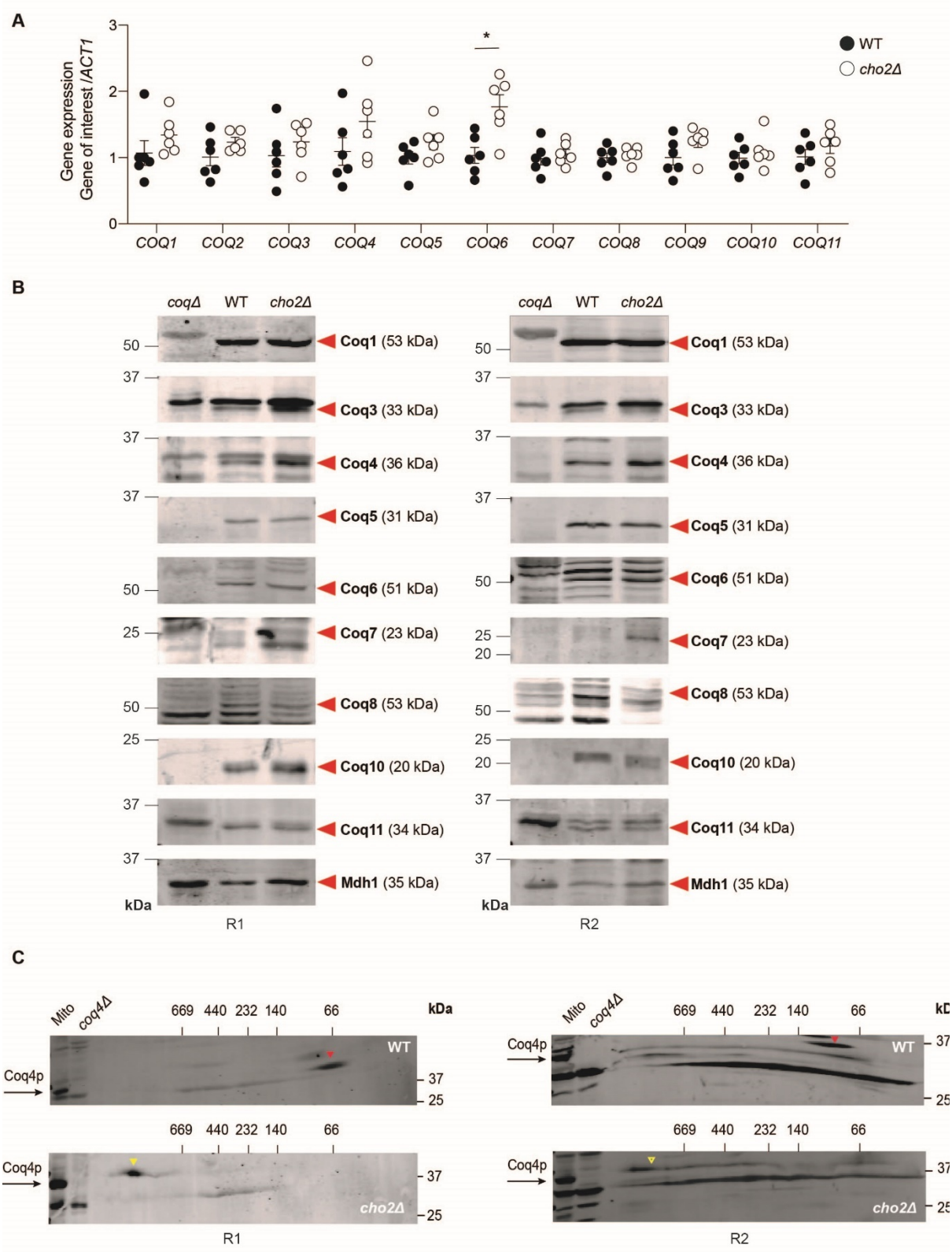

Fig. S5. Increased CoQ_6 in *cho2Δ* cannot be explained by changes in the expression of the CoQ biosynthetic pathway. (**A**) Gene expression of the CoQ biosynthetic genes in *cho2Δ* mutants compared to WT as determined by qPCR (n=6). (**B**) Protein levels of the CoQ biosynthetic pathway in isolated mitochondria from WT and *cho2Δ* as measured by Western blotting (n=3), representative image shown. (**C**) Two-dimensional Blue Native/SDS PAGE separation and immunoblotting of the high molecular weight CoQ synthome protein complex in WT and *cho2Δ*. (n=3), representative image shown. Red arrow indicates low molecular mass species in WT and the yellow arrow indicates an increase in a high molecular weight species in *cho2Δ*. Data and error bars depict mean ± s.e.m. *P ≤ 0.05 as determined by Kruskal-Wallis test (**A**). **B** and **C** show results of two independent replicates (R1 and R2).

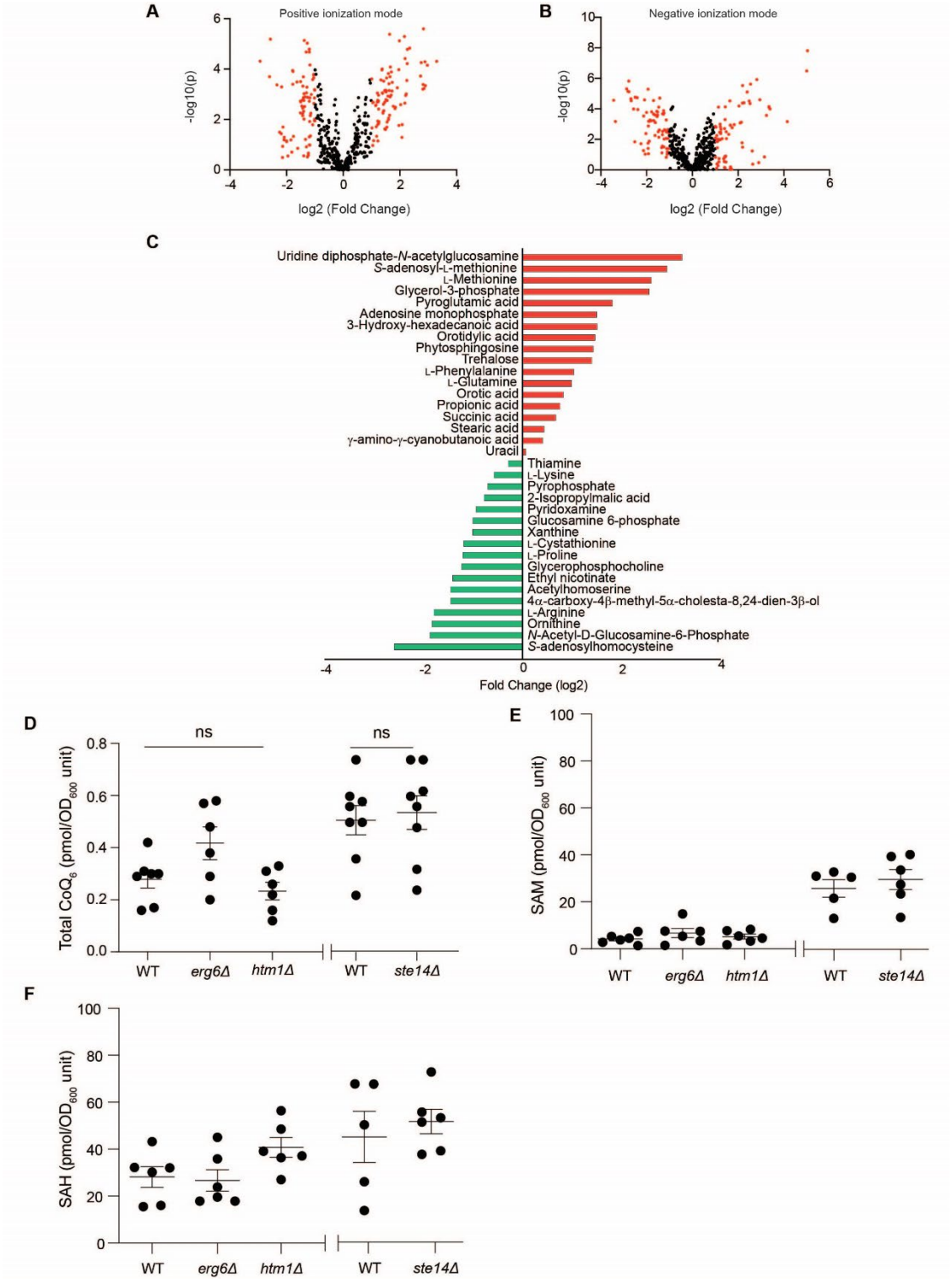

Fig. S6. Untargeted metabolomics analyses of WT and *cho2Δ* reveal *S*-adenosylmethionine (SAM) and *S*-adenosylhomocysteine (SAH) alterations. (**A-B**), Volcano plots indicating significantly alerted metabolites (red) in *cho2Δ* versus WT cells in both positive and negative ionization modes. Data taken from n=5. (**C**) Metabolites significantly altered in *cho2Δ* versus WT cells. Data taken from n=5. (**D**) CoQ_6 content in yeast methyltransferase mutants *erg6Δ, htm1Δ* and *ste14Δ* (n=6). (**E**) SAM content in yeast methyltransferase mutants *erg6Δ, htm1Δ* and *ste14Δ* versus their respective WT cells (n=6). (**F**) SAH content in yeast methyltransferase mutants *erg6Δ, htm1Δ* and *ste14Δ* versus their respective WT cells (n=6). The *erg6Δ* and *htm1Δ* strains were in the BY4743 background and compared to BY4743 WT for all studies. The *ste14Δ* used was in the BY4741 background and compared to BY4741 WT for all studies. Data and error bars in **D-F** depict mean ± s.e.m. *P ≤ 0.05 and ns indicates 'not significant' as determined by Mann-Whitney (*ste14Δ*) or Kruskal-Wallis test (*erg6Δ* and *htm1Δ*).

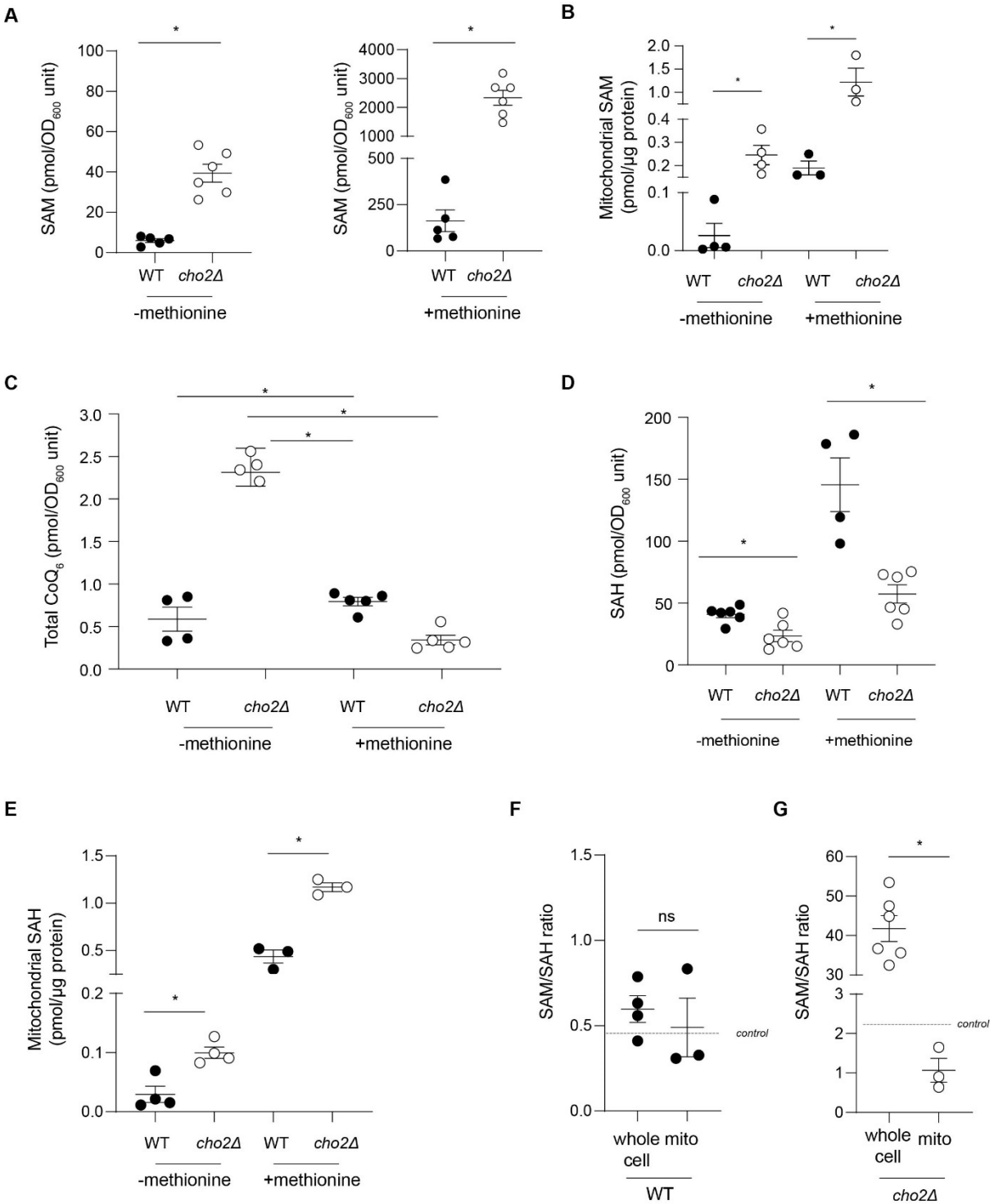

Fig. S7. Treatment with methionine drives changes in the mitochondrial SAM-to-SAH ratio in *S. cerevisiae*. (**A**) Whole-cell SAM content in WT and *cho2Δ* grown in the presence or absence of 1 mM methionine (n=3-4). (**B**) Mitochondrial SAM content in WT and *cho2Δ* grown in the presence or absence of 1 mM methionine (n=3)**.** (**C**) CoQ_6 content in WT and *cho2Δ* grown in the presence or absence of 1 mM methionine (n=4-5). (**D**) Whole-cell SAH content in WT and *cho2Δ* grown in the presence or absence of 1 mM methionine (n=3-4). (**E**) Mitochondrial SAH content in WT and *cho2Δ* grown in the presence or absence of 1 mM methionine (n=3). (**F**) Whole-cell and mitochondrial SAM/SAH ratios in WT cells treated with 1 mM methionine (n=3-4). (**G**) Whole-cell and mitochondrial SAM/SAH ratios in *cho2Δ* cells treated with 1 mM methionine (n=3-4). In **E** and **G**, dotted line represents untreated (control) values of respective strains. Data and error bars depict mean ± s.e.m. *P ≤ 0.05 and ns indicates 'not significant' as determined by Mann-Whitney (**F-G**) or Kruskal-Wallis test (**A-E**).

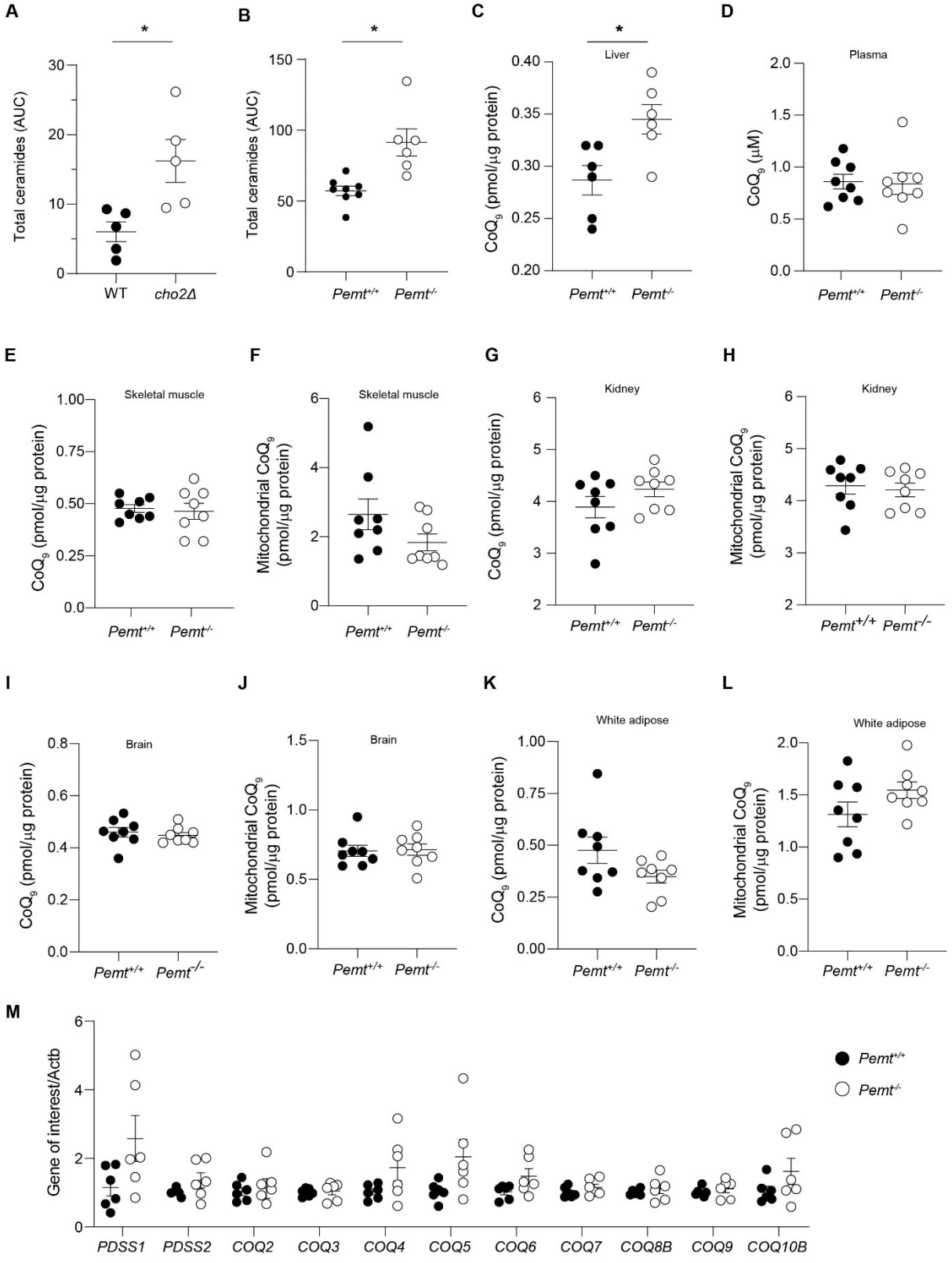

Fig. S8. Pemt deficiency selectively increases liver CoQ in mice fed chow diet. (**A**) Total ceramide species in WT and *cho2Δ*. **(B)** Total hepatic ceramide species in $Pemt^{+/+}$ and $Pemt^{-/-}$ mice. **(C)** Total hepatic CoQ_9 content in $Pemt^{+/+}$ and $Pemt^{-/-}$ mice fed chow (n=6). (**D**) Plasma CoQ_9 content in $Pemt^{+/+}$ and $Pemt^{-/-}$ mice fed chow (n=8). (**E-F**) Total and mitochondrial CoQ_9 content in skeletal muscle (n=8). (**G-H**) Total and mitochondrial CoQ_9 content in kidney (n=8). (**I-J**), Total and mitochondrial CoQ_9 content in brain (n=8). (**K-L**) Total and mitochondrial CoQ_9 content in white adipose tissue (n=8). (**M**) Hepatic gene expression of the CoQ biosynthetic pathway in $Pemt^{+/+}$ and $Pemt^{-/-}$ mice fed chow as determined by qPCR (n=6). Data and error bars depict mean ± s.e.m. $*P \leq 0.05$ as determined by Mann-Whitney (**A-J**) or Kruskal-Wallis test (**K**).

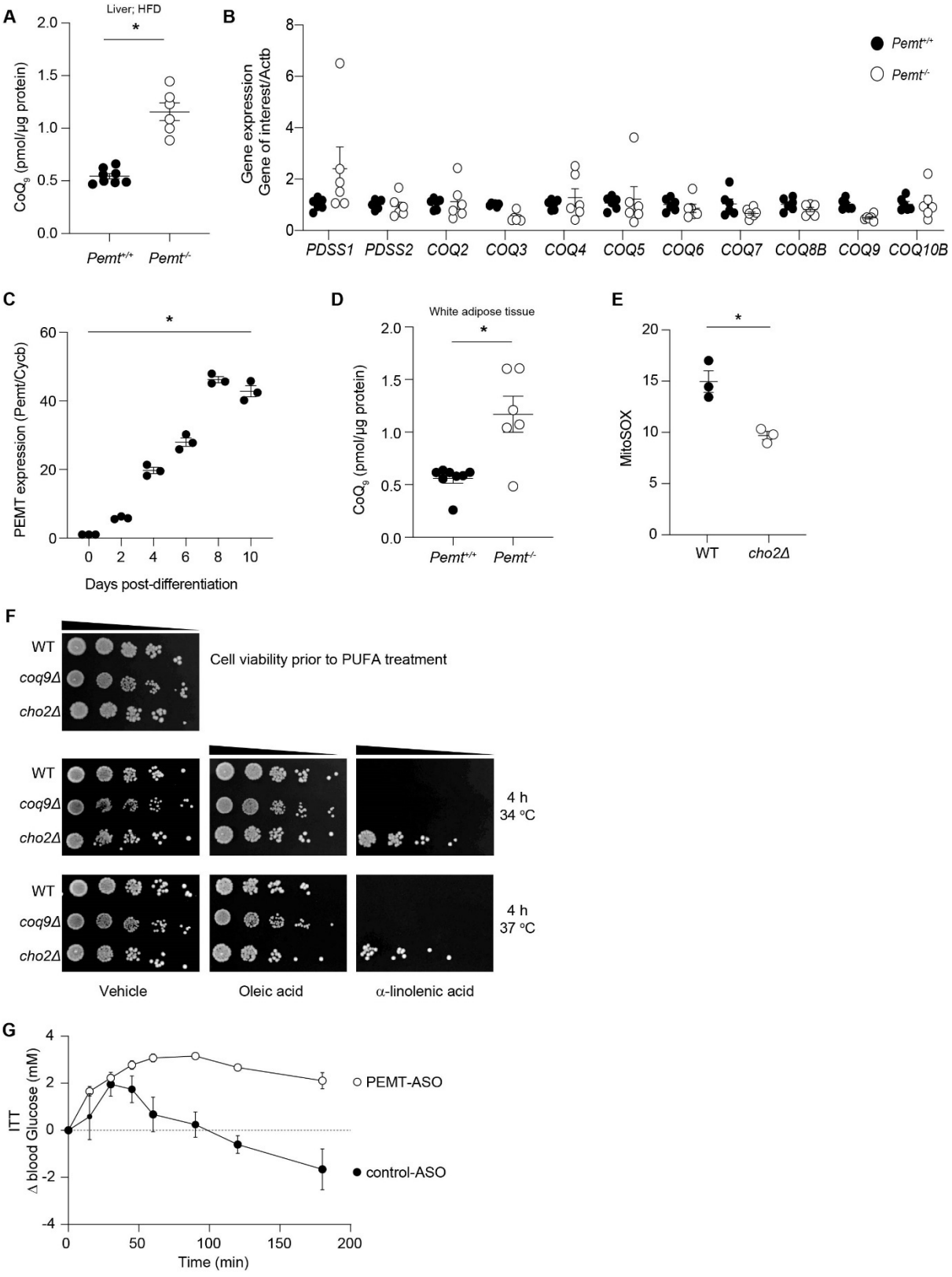

Figure S9. Pemt deficiency in mice fed a high-fat diet (HFD) and effect on mitochondrial superoxide production. (**A**) Total hepatic CoQ_9 content in *Pemt*$^{+/+}$ and *Pemt*$^{-/-}$ mice a HFD for 6 weeks (n=6-8). (**B**) Hepatic gene expression of the CoQ biosynthetic pathway in *Pemt*$^{+/+}$ and *Pemt*$^{-/-}$ mice fed HFD for 6 weeks as determined by qPCR (n=6). (**C**) PEMT gene expression as measured by qPCR during differentiation in 3T3-L1 adipocytes (n=3). (**D**) Total CoQ_9 content in white adipose tissue in *Pemt*$^{+/+}$ and *Pemt*$^{-/-}$ mice fed HFD for 6 weeks (n=6-8). (**E**) Mitochondrial superoxide content in *cho2Δ* compared to WT cells as measured by MitoSOX fluorescence (n=3)**.** (**F**) Polyunsaturated fatty acid stress assay induced by α-linolenic acid at elevated temperatures in WT and *cho2Δ*. Oleic acid was used as a monounsaturated fatty acid control, and *coq9Δ* as a CoQ deficient control strain. Representative image of three independent replicates shown. **(G)**

Baseline (0 min) corrected blood glucose concentrations (Δ blood glucose) in C57BL/6J mice fed HFD treated with either control or anti-PEMT ASO for 10 weeks. Δ blood glucose concentrations were determined over three hours post insulin challenge with inversed values plotted. Dotted line indicates baseline. Data is mean of n=5-10 mice per group. Data and error bars depict mean ± s.e.m. $*P \leq 0.05$ as determined by Mann-Whitney (**A, D, E**) or Kruskal-Wallis test (**B, C**).

Materials and Methods

Methods

Yeast strains

See Table S2 for details of *Saccharomyces cerevisiae* (*S. cerevisiae*) strains used in this study. For the genome-wide screen and subsequent experiments, *S. cerevisiae* homozygous diploid BY4743 WT and corresponding knockout mutants were used. For selected experiments where haploid yeast strains were required, yeast from the BY4741 or W303a backgrounds were used. BY4743 *CHO2* heterozygous diploid strain was constructed by crossing BY4741 *cho2Δ* with BY4742 WT using standard yeast techniques (17). *CHO2* was disrupted in W3031a using a one-step gene replacement method using the nourseothricin antibiotic resistance cassette from *pFA6a*–natNT2 (18). For *CHO2* knockout (*CHO2*-S1 and *CHO2*-S2) and verification primers (*CHO2*-A and *CHO2*-D) see Table S3. Rho^0 strains were generated by growth of WT cells in medium containing 10 mg/mL ethidium bromide for two rounds of growth. Respiratory incompetence was verified by comparison of growth on media containing glucose (2% w/w) with medium containing glycerol (3% w/v). Cells that grew on glucose but not glycerol containing medium were considered respiratory incompetent.

Yeast cell growth

For all experiments, yeast cells were recovered from -80 °C glycerol stocks in YEPD liquid (2% glucose, 1% yeast extract, 2% peptone) or YEPD agar (YEPD plus 2% bacteriological agar) for 2 d at 30 °C. Subsequently, all growth was carried out in synthetic defined medium lacking the CoQ head-group precursors 4-hydroxybenzoic acid (4HB) and *para*-aminobenzoic acid (pABA) (SD-4HB-pABA; 2% glucose or galactose, 6.7% yeast nitrogen base + nitrogen lacking 4-hydroxybenzoic acid and *para*-aminobenzoic acid (Sunrise Scientific #1563-100)) supplemented with appropriate amino acids and bases (1.3% leucine, 0.9% lysine, 0.38% isoleucine, 0.60% valine, 0.23% histidine, 0.45% tryptophan, 0.275% adenine, 0.11% uracil (w/v)) unless otherwise indicated. Cells were grown at 30 °C with shaking until cell biomass reached OD_{600} ~1.0 or as indicated. Cell cultures were harvested by centrifugation (17,000 x *g*; 10 min; 4 °C) and cells were used immediately or stored at -20 °C until further use.

Construction of constitutive low-copy CHO2 yeast expression vector and expression in yeast

A constitutive low-copy *CHO2* containing plasmid was constructed using the pAG416-GPD vector backbone donated kindly by Prof. Anthony Cooper (Garvan Medical Research Institute). The *CHO2* open reading frame was cloned into pAG416-GPD using Gibson Assembly (New England Biolabs; see Table S3 for primers *CHO2*-F and *CHO2*-R). Clones were sequenced by Sanger sequencing, and positive clones were transformed into BY4743 WT and *cho2Δ* yeast,

along with the corresponding empty vector (pAG416-GPD) control using the lithium acetate method (19). Yeast cells were grown using media lacking uracil to maintain selection pressure.

Overexpression of mitochondrial-targeted SAM1 in yeast

Plasmids expressing cytosolic *SAM1* (SAM1-pYES2) and mitochondrial-targeted *SAM1* (Su9(1–69)-*SAM1*-pYES2) (20) were kindly donated by Dr. Agrimi (University of Bari). SAM1-pYES2 and Su9(1–69)-SAM1-pYES2 were transformed into BY4743 WT and *cho2*Δ yeast, along with the corresponding empty vector (pYES2) control using the Li-acetate transformation method (19). Yeast cells were grown using media lacking uracil to maintain selection pressure.

Transcriptomic analyses

Yeast cultures were grown overnight in SD-4HB-pABA. Pre-cultures were diluted and grown overnight with shaking (30 °C) until cell density reached OD_{600} ~1.0 in SD-4HB-pABA. For experiments involving CoQ_6 supplementation, cells were grown in the presence of 10 μM CoQ_6. Cell were harvested at OD_{600} ~1.0 cell pellets were store at -20 °C until analyses. RNA was extracted from cells using TRIzol reagent (Invitrogen) and DNA contamination was removed using the DNase TURBO kit as per manufacturer's instructions (Invitrogen). RNA concentration was measured by Nanodrop (ThermoFisher Scientific) and RNA was stored at -20ºC. RNA quality was determined by spectrophotometry (Nanodrop) and by Bioanalyser (Ramaciotti Centre for Gene Function Analysis, University of New South Wales, Australia). Preparation of cRNA, probes, and hybridization to whole yeast genome microarrays (YG-S98, Affymetrix) was performed at the Ramaciotti Centre. Candidate differentially expressed genes with a significant Bonferroni adjusted p value < 0.05 and fold-change > 2.0 (mutant versus WT) were identified using *limma* R package (21) after normalization by robust-multiarray average (MRA) algorithm from *affy* R package (22).

Rate of CoQ_6 synthesis

For determination of CoQ_6 synthesis rates, WT and *cho2Δ* cells were grown in SD-4HB-pABA (30 °C shaking) until OD_{600} ~0.5 and then either $^{13}C_6$-4-hydroxybenzoic acid (Cambridge isotope, USA) or unlabelled 4-hydroxybenzoic acid was added to a final concentration of 200 μg. Cell were harvested at OD_{600} ~1.0 and 2.0 and cell pellets were store at -20 °C until analyses. On the day of analysis, cells were defrosted and CoQ_6 and $^{13}CoQ_6$ were extracted from yeast cells using acidified methanol and hexane as described above and 2 μL injected onto an Agilent 1290 UHPLC system connected to an Agilent 6490 triple-quadrupole mass spectrometer with column, mobile phases, gradient elution, flow rate and mass spectrometry parameters as above. MRM settings for $^{13}C_6$-CoQ_6 (parent ion→fragment ion) were *m/z*

597.3→ 203.1 with collision energy (CE) = 33 V. $^{13}C_6$-CoQ_6 was quantified against authentic CoQ_6 commercial standard and rate of synthesis determined.

CoQ_6 content in yeast mitochondria

Yeast cultures of WT BY4743 and *cho2Δ* were grown overnight. Pre-cultures were diluted and grown overnight with shaking (30 °C) until cell density reached OD_{600} ~1.0. Spheroplasts were prepared with Zymolyase-20T (MP Biomedicals) and fractionated as previously described (23) in the presence of cOmplete™ EDTA-free protease inhibitor cocktail tablets (Roche), phosphatase inhibitor cocktail set I (Sigma-Aldrich), phosphatase inhibitor cocktail set II (Sigma-Aldrich) and phenylmethylsulfonyl fluoride (PMSF). Purified mitochondria were frozen in liquid nitrogen, aliquoted, and stored at -80 °C until analyses. Protein concentration of mitochondria was measured by the bicinchoninic acid (BCA) assay (ThermoFisher Scientific). On the day of analysis, mitochondrial extracts were defrosted, and lipid extracted in the presence of internal standard CoQ_4 and analyzed for CoQ_6 by LC-MS/MS as previously described (16).

Mitochondrial DNA determination

Mitochondrial DNA estimation was carried out as previously described (3). Briefly, yeast cells at OD_{600} ~1.0 were collected by centrifugation at 3000 x *g* for 5 min, washed with H_2O, and frozen at -20 °C until DNA extraction was carried out. Cell pellets were resuspended in 200 µL lysis buffer (10 mM Tris-Cl pH 8.0, 2% (v/v) Triton X-100, 1 mM EDTA, 100 mM NaCl, 1% SDS), and 200 µL acid-washed glass beads and 200 µL of phenol:chloroform:isoamyl alcohol (25:24:1) were added to the cell suspension. Cells were lysed using a bead-beater (Precellys 24; Bertin Technologies) for 3 x 10 s at 6500 rpm with a 45 s break between rounds at 4ºC. 200 µL of Tris-EDTA (TE) buffer (10 mM Tris-Cl, 1 mM EDTA) was added and cell suspension was centrifuged at 13,000 x *g* for 5 min at room temperature. The aqueous layer was removed to a new tube containing 200 µL of chloroform, mixed by inversion and centrifuged at 13,000 x *g* for 5 min at room temperature. This was repeated once more. After this, the aqueous layer was transferred to a 2 mL screw-cap tube containing 1 mL of 95% ethanol, mixed by inversion, and centrifuged at 13,000 x *g* for 2 min at room temperature. The resulting pellet was resuspended in 400 µL of TE containing 30 µg RNase A and incubated at 37ºC for 30 min. 10 µL of 3 M sodium acetate and 1 mL of 95% ethanol was added, mixed by inversion, and incubated at -20ºC for 1 h. After 1 h of incubation at -20ºC, the suspension was centrifuged at 13,000 x *g* for 5 min and the pellet washed twice with 70% v/v ethanol and air dried. The dried pellet was resuspended in 25 µL of TE and concentration measured by Nanodrop (ThermoFisher Scientific) and stored at -20 °C until use.

qPCR was performed on a CFX384 instrument (Bio-Rad) using the SensiFAST™ SYBR® No-ROX kit (Bioline) as per the manufacturer's instructions. Each sample was run in duplicate with 150 ng of total DNA used per reaction using the following thermocycling protocol (95 °C for 2 min, 95 °C for 5 s, 60 °C for 10 s, and 72 °C for 20 s, plate read and cycle repeated X40, melt curve 40 –92 °C with plate read and 40 °C for 10 s). Melting curve analysis confirmed that all PCRs produced a single product. mtDNA-specific primers and actin-specific primers were used (see Table S3 for primers mtDNA_F, mtDNA_R, ACT1F and ACTR*).* The relative level of gene expression of mitochondrial DNA was normalised to the level of actin as described previously (24).

Citrate synthase activity

The measurement of citrate synthase activity in yeast cells was carried out as described previously (25). Briefly, yeast cells at approximately OD_{600} ~1.0 were collected by centrifugation at 3,000 x *g* for 5 min, washed with H_2O, and frozen at -20 °C until activity assays were carried out. On the day of analysis, cell pellets were defrosted and resuspended in 200 µL lysis buffer (100 mM Tris-Cl pH 7.4, 1% (v/v) Triton X-100, 1 mM EDTA, 1 mM phenylmethylsulfonyl fluoride, 1 x cOmplete™ Protease Inhibitor Cocktail (Roche)), with 200 µL acid-washed glass beads. Cells were lysed using a bead-beater (Precellys 24; Bertin Technologies) for 3 x 10 s at 6500 rpm with a 45 s break between rounds at 4 °C. The clarified cell lysate was collected after centrifugation at 16,000 x *g* for 10 min at 4 °C. Bicinchoninic acid assay (ThermoFischer Scientific) was done to quantify the protein concentration. Cell lysates were normalized to 0.05 µg/uL protein. The citrate synthase assay was carried out using a VersaMax plate reader (Molecular Devices) in a flat-bottom 96 well plate. 40 µL of 500 mM Tris-Cl pH 7.4, 2 µL of 30 mM acetyl CoA, 8 µL of 2.5 mM 5,5'- dithio-*bis*(2-nitrobenzoic acid) (DTNB), 90 µL H_2O, and 50 µL cell lysate (2.5 µg total protein), were added into each well. 10 µL of 10 mM oxaloacetic acid was added per well and mixed by pipetting up and down. Absorbance at 412 nm (A_{412}) was measured every 30 s at 25 °C. The initial slope was calculated by using data from the first 10 min and used to determine the enzyme reaction rate using the extinction coefficient for TNB of 14.15 mM^{-1} cm^{-1} (26).

Quantitative real-time PCR (qRT-PCR)

Total RNA was isolated from cells or tissue using TRIzol reagent (Invitrogen). For yeast RNA, DNA contamination was removed using the DNase TURBO kit as per manufacturer's instructions (Invitrogen). RNA concentration was measured by Nanodrop (ThermoFisher Scientific) and RNA was stored at -20 °C. Reverse transcription was carried out using the Superscript III first strand synthesis system using random hexamer primers (Invitrogen). cDNA was stored at -20 °C until qPCR analyses were carried out. Quantitative real-time PCR was

performed on a CFX384 instrument (BioRad) using the SensiFAST™ SYBR® No-ROX kit (Bioline) in duplicate. The relative levels of gene expression were normalized to the expression level of actin or cyclophilin D as indicated. Melting curve analysis confirmed that all PCR reactions produced a single product. The primers (forward/reverse) used in real-time PCR were designed using Primer3 online (http://bioinfo.ut.ee/primer3/) for yeast primers or the PrimerBank database (https://pga.mgh.harvard.edu/primerbank/index.html) for mouse primers. All primers used are listed in Table S3.

Determination oxygen consumption in yeast cells using high-resolution respirometry

High resolution respirometry to determine basal and maximal oxygen consumption rates was carried out using an Oroboros O2k Oxygraph system. WT and *cho2*Δ yeast cells were grown until OD_{600} ~1.0. 1 OD of cells were harvested by centrifugation (17,000 x *g*; 10 min; 4 °C) and resuspended in 6 mL of fresh medium. Each chamber of the Oroboros O2k Oxygraph was filled with 3 mL of cell suspension and the stoppers carefully inserted to ensure no air bubbles remained in the chamber. Routine/basal respiration was acquired by allowing the cells to equilibrate in the chambers until a steady reading was reached and oxygen consumption recorded. Mitochondrial membrane potential was then collapsed to acquire maximal flux through the electron transfer system by three sequential addition of 10 mM 2-[[4-(trifluoromethoxy)phenyl]hydrazinylidene]propanedinitrile (FCCP). Residual oxygen flux was then acquired by the addition of 1 M sodium azide. Each sample was measured in technical duplicate.

SDS-PAGE and immunoblot analysis

Whole cell immunoblot - Briefly, yeast cells at OD_{600} ~1.0 were collected by centrifugation at 3000 x *g* for 5 min, washed with H_2O, and frozen at -20 °C until protein extraction was carried out. For protein extraction, cell pellets were resuspended in Thorner buffer (40 mM Tris-Cl pH 8.0, 5% w/v SDS, 8 M urea, 100 µM EDTA, 1 mM phenylmethylsulfonyl fluoride, 1 x cOmplete™ Protease Inhibitor Cocktail (Roche)), and 200 µL acid-washed glass beads were added. Cells were lysed using a bead-beater (Precellys 24; Bertin Technologies) for 3 x 10 s at 6500 rpm with a 45 s break between rounds at 4 °C. The clarified cell lysate was collected after centrifugation at 17,000 x *g* for 10 min at 4 °C. BCA assay (ThermoFischer Scientific) was done to quantify protein concentration. 20 µg of protein were resuspended in SDS sample buffer (50 mM Tris-Cl pH 6.8, 2% w/v SDS, 0.1% bromophenol blue, 10% (v/v) glycerol, 100 mM DTT) and separated by SDS gel electrophoresis on 10% NuPAGE Bis-Tris gels (Thermo Fischer Scientific) using MOPS running buffer (50 mM MOPS, 50 mM Tris Base, 0.1% SDS, 1 mM EDTA pH 7.7). Proteins were transferred to nitrocellulose membrane using the iBlot2 system (Thermo Fischer Scientific) using Program 0 and then blocked using 10% skim milk

and 0.05% Triton X-100 in Tris-buffered saline for 1 h at room temperature. Porin and actin (antibody dilutions in Table S4) were probed with mouse monoclonal antibodies prepared in 5% skim milk and 0.05% Triton X-100 in Tris-buffered saline overnight at 4 °C. Anti-mouse IgG secondary antibody (Dako) was used at dilution of 1:10,000 in 5% skim milk and 0.05% Triton X-100 in Tris-buffered saline for 1 h at room temperature. Proteins were visualized on film using chemiluminescent detection. Immunoblots are representative of six replicates and were quantified by hand using ImageStudio Lite software with porin content normalized to actin.

Isolated mitochondria immunoblot—Purified mitochondria (25 μg) were resuspended in SDS sample buffer and separated by SDS gel electrophoresis on 10% or 12% Tris-glycine polyacrylamide gels. Proteins were transferred to 0.45 μm PVDF membrane (Millipore) and blocked with blocking buffer (0.5% BSA, 0.1% Tween 20, 0.02% SDS in phosphate-buffered saline). Representative Coq polypeptides and loading control mitochondrial malate dehydrogenase (Mdh1) were probed with rabbit polyclonal antibodies prepared in blocking buffer at dilutions listed in Table S4. IRDye 680LT goat anti-rabbit IgG secondary antibody (LiCOR) was used at a dilution of 1:10,000. Proteins were visualized using a LiCOR Odyssey Infrared Scanner (LiCOR). Immunoblots are representative of three replicates and were quantified by hand using ImageStudioLite software normalized to Mdh1.

Two-dimensional Blue Native/SDS-PAGE immunoblot analysis of high molecular weight complexes

Two-dimensional Blue Native (BN)/SDS-PAGE was performed as described (27-29). Briefly, 200 μg of purified mitochondria were solubilized at 4 mg/mL for one hour on ice with 16 mg/mL digitonin (Biosynth) in the presence of the protease and phosphatase inhibitors used during mitochondrial isolation. Protein concentration of solubilized mitochondria was determined by BCA assay. NativePAGE 5% G-250 sample additive (ThermoFisher Scientific) was added to a final concentration of 0.25%. 80 μg of solubilized mitochondria were separated on NativePAGE 4-16% Bis-Tris gels (ThermoFisher Scientific) in the first dimension, and native gel slices were further separated on 12% Tris-glycine polyacrylamide gel in the second dimension. Following the second-dimension separation, immunoblot analyses were performed as described above, using antibodies against Coq4 at the dilutions indicated in Table S4. Molecular weight standards for BN gel electrophoresis and SDS gel electrophoresis were obtained from GE Healthcare (Sigma-Aldrich) and Bio-Rad, respectively

Phosphatidylcholine, dolichol and triacylglyceride extraction from yeast cells

100 μL of 50% methanol containing 100 μM DTPA was added to harvested cell pellets and barocycled at 40 kpsi (50 s on, 10 s off for 30 cycles at 20 °C) using a Barocycler 2320EXT

(Pressure BioSciences Inc). Cell lysates were transferred to microcentrifuge tubes and 50 µL butylated hydroxytoluene, 2.5 µL internal standard diluted in methanol (SPLASH® LIPIDOMIX® Mass Spec Standard; Sigma-Aldrich), 380 µL 50% methanol and 250 µL chloroform added. Samples were vortexed vigorously for 1 min at room temperature and then centrifuged at 17,000 x *g* for 10 min at 4 °C. 200 µL of chloroform was removed and transferred to an LC/MS vial. 250 µL of chloroform added to the sample, vortexed vigorously for 1 min at room temperature and then centrifuged at 17,000 x *g* for 10 min at 4 °C. 250 µL of chloroform was removed and combined with the first 200 µL aliquot removed. Chloroform was dried under nitrogen and dried lipids were stored at -80 °C until analyses. Prior to analyses, dried lipids were resuspended in 100 µL of chloroform:methanol (1:1, vol:vol) and subjected to LC/MS analysis as outlined below.

Lipid analyses by LC-MS/MS

Lipid analysis of yeast extracts was performed as described previously (30) using an Agilent 6560 Ion Mobility Q-TOF LC/MS coupled to a 1290 Infinity II UPLC system. Lipids were separated on Waters Acquity CSH C18 column (1.7 µm, 100 mm x 2.1 mm). 5 µL of lipid extract was subjected for LC/MS analysis. Column was kept at 55 °C and elution gradient consisted of mobile phase A (water/acetonitrile, 4:6, v/v) with 10 mM ammonium formate and mobile phase B (acetonitrile/2-propanol, 1:9, v/v) with 10 mM ammonium formate. The flow rate was 0.3 mL/min and the gradient ran from 0 to 40% mobile phase B in the first 6 min, increased to 100% mobile phase B in the next 24 min, kept at 100% mobile phase B for further 4 min, and returned to 0% mobile phase B over 2 min followed by column equilibration for another 4 min (total run time of 40 min). Lipids were analyzed in positive ionization polarity mode with electrospray settings as follows: gas temperature 300 °C, drying gas flow 5 L/min, sheath gas temperature 300 °C; sheath gas flow 12 L/min; cap voltage 3.5 kV. Auto MS/MS mode was used to acquire data with scan range of 100-1700 m/z and collision energy 35 eV. M/z 121.0509 and m/z 922.0098 ions were used as "lock masses" and were introduced by constant infusion of reference calibration solution. Peak detection and peak area integration were performed using Mass Hunter Workstation Software (Agilent Technologies, USA). Identification of lipid species were performed using acquired MS/MS data and LipidMatch software (31).

MitoSOX measurements

Yeast cells at OD_{600} ~1.0 were collected by centrifugation at 3000 x *g* for 1 min, washed with phosphate buffered saline (PBS) twice and resuspended in PBS for a final concentration of 1 OD unit. MitoSOX was added to the yeast suspension (5 µM end concentration; 50 µM stock made in PBS). Cells were incubated in the dark at 30 °C for 45 min with gentle shaking. After

45 min, cells were washed twice in PBS, resuspend in fresh PBS and pipetted into a black multi-well plate. Fluorescent was measured using a PHERAStar FSX (BMG Lab Tech) with a 510/580 nm (ex/em) detector as per Manufacturer's instructions.

Fatty acid sensitivity assay

Sensitivity of yeast cells to PUFA-induced oxidative stress was performed as described previously (3). Briefly, cells were grown overnight at 30 °C shaking. Cultures were sub-inoculated to an OD_{600}= 0.25 in fresh medium and incubated at 30 °C, shaking until cells reached OD_{600} ~1.0. Cells were harvested, washed twice with sterile water, and diluted in 0.1 M phosphate buffer with 0.2% dextrose, pH 6.2, to an OD_{600} = 0.2. The cell suspension was divided into 5-ml aliquots and treated with an ethanol vehicle control (final concentration 0.1% v/v), ethanol-diluted oleic acid (Nu-Check Prep), or α-linolenic acid (Nu-Check Prep) to a final concentration of 200 µM. Fatty acid-treated cultures were incubated for 4 h at 30 °C shaking, after which cell viability was assessed via plate dilutions. Cell viability prior to the addition of fatty acids was determined via plate dilutions, represented in the 0-h plate.

PEMT knockdown in 3T3-L1 adipocyte via anti-sense oligonucleotide (ASO) treatment

At 6-7 days post differentiation, 3T3-L1 adipocytes were transfected with control scrambled and anti-PEMT antisense oligonucleotides (ASO; Ionis Pharmaceuticals Inc.) as per *in vivo* mouse studies. To transfect cells, 300 nmol ASO, 7.5 µL Trans-ITX2 Dynamic delivery system and 100 µL of OptiMEM (per 12-well) were combined and incubated at room temperature for 30 min. During this incubation time, 3T3-L1 adipocytes were trypsinized (5x trypsin, EDTA; Thermo Fisher Scientific) at 37°C and centrifuged at 120 x *g* for 5 min at room temperature. Adipocytes were resuspended in DMEM/10% FCS/GlutaMAX and the appropriate ASO-solution added. Cells were seeded onto Matrigel (Corning) coated plates and grown for 4 d. Pemt knockdown by ASO treatment was verified using qPCR.

TNFα treatment of in 3T3-L1 adipocytes

Insulin resistance was induced by tumor necrosis factor-α (TNFα) in 3T3-L1 adipocytes as previously described (32). At 6-7 days post differentiation, 3T3-L1 adipocytes were incubated with 2 ng/mL TNFα (R&D Systems) diluted in phosphate buffered saline for 4 d. Medium was changed every 24 h and replaced with fresh medium containing 2 ng/mL TNFα.

CoQ synthesis inhibition in 3T3-L1 adipocytes

At 6-7 days post differentiation, 3T3-L1 adipocytes were treated with 1 mM 4-nitrobenzoic acid made in DMEM/10% FCS/GlutaMAX to inhibit CoQ synthesis (33). Medium was changed every 24 h and replaced with fresh medium containing 1 mM 4-nitrobenzoic acid.

2-Deoxyglucose (2-DOG) uptake assays in cultured cells

2-Deoxyglucose (2-DOG) uptake was measured as previously described (7). 3T3-L1 cells were differentiated and grown as outlined above in 24-well plates. To measure 2-DOG uptake, cells were serum starved for 2 h in DMEM/0.2% BSA/1% GlutaMAX at 37ºC/5% CO_2. Cells were washed and incubated in pre-warmed (37ºC) Krebs–Ringer phosphate (KRP) buffer (0.6 mM Na_2HPO_4, 0.4 mM NaH_2PO_4, 120 mM NaCl, 6 mM KCl, 1mM $CaCl_2$, 1.2 mM $MgSO_4$ and 12.5 mM HEPES (pH 7.4) containing 0.2% bovine serum albumin and 24-well plates transferred to a 37 ºC water bath for the assay. Cells were stimulated with 100 nM insulin for 20 min and 25 mM cytochalasin B (Sigma Aldrich) was added as a control to determine non-specific 2-DOG uptake to the wells before addition of 2-[^{3}H]deoxyglucose (PerkinElmer). During the final five min, tritiated 2-DOG (0.025 mCi, 50 mM) was added to cells to measure steady-state rates of labelled 2-DOG uptake. Following three washes with ice-cold PBS, cells were solubilized in PBS containing 1% (v/v) Triton X-100. Tracer uptake was quantified by liquid scintillation counting (Packard Tri-Carb β-scintillation counter using Optima XR scintillation fluid, Perkin Elmer). Samples were read for 5 min and Disintegrations Per Minute (DPM) used for data analysis. Data was normalized for protein content and further normalized to Δ glucose uptake (insulin treated minus control values).

Statistical analyses

All statistical analyses were carried out using GraphPad Prism V8.

References

1. Brachmann CB, Davies A, Cost GJ et al. Designer deletion strains derived from *Saccharomyces cerevisiae* S288C: a useful set of strains and plasmids for PCR-mediated gene disruption and other applications. *Yeast* 1998;14:115-32.
2. Winzeler EA, Shoemaker DD, Astromoff A et al. Functional characterization of the *S. cerevisiae* genome by gene deletion and parallel analysis. *Science* 1999;285:901-6.
3. Bradley MC, Yang K, Fernández-Del-Río L et al. *COQ11* deletion mitigates respiratory deficiency caused by mutations in the gene encoding the coenzyme Q chaperone protein Coq10. *J. Biol. Chem.* 2020;295:6023-42.
4. *Saccharomyces* Genome Deletion Project Consortium. http://www-sequence.stanford.edu/group/yeast_deletion_project/deletions3.html 2007.
5. Santos JH, Mandavilli BS, Van Houten B. Measuring oxidative mtDNA damage and repair using quantitative PCR. *Methods Mol. Biol.* 2002;197:159-76.
6. Croft KD, Zhang D, Jiang R et al. Structural requirements of flavonoids to induce heme oxygenase-1 expression. *Free Radic. Biol. Med.* 2017;113:165-75.
7. Fazakerley DJ, Chaudhuri R, Yang P et al. Mitochondrial CoQ deficiency is a common driver of mitochondrial oxidants and insulin resistance. *eLife* 2018;7:e32111.
8. Gin P, Clarke CF. Genetic evidence for a multi-subunit complex in coenzyme Q biosynthesis in yeast and the role of the Coq1 hexaprenyl diphosphate synthase. *J. Biol. Chem.* 2005;280:2676-81.
9. Hsieh EJ, Gin P, Gulmezian M et al. *Saccharomyces cerevisiae* Coq9 polypeptide is a subunit of the mitochondrial coenzyme Q biosynthetic complex. *Arch. Biochem. Biophys.* 2007;463:19-26.
10. Poon WW, Barkovich RJ, Hsu AY et al. Yeast and rat Coq3 and *Escherichia coli* UbiG polypeptides catalyze both *O*-methyltransferase steps in coenzyme Q biosynthesis. *J. Biol. Chem.* 1999;274:21665-72.
11. Belogrudov GI, Lee PT, Jonassen T, Hsu AY, Gin P, Clarke CF. Yeast *COQ4* encodes a mitochondrial protein required for coenzyme Q synthesis. *Arch. Biochem. Biophys.* 2001;392:48-58.
12. Baba SW, Belogrudov GI, Lee JC et al. Yeast Coq5 C-methyltransferase is required for stability of other polypeptides involved in coenzyme Q biosynthesis. *J. Biol. Chem.* 2004;279:10052-9.
13. Gin P, Hsu AY, Rothman SC et al. The *Saccharomyces cerevisiae COQ6* gene encodes a mitochondrial flavin-dependent monooxygenase required for coenzyme Q biosynthesis. *J. Biol. Chem.* 2003;278:25308-16.
14. Tran UC, Marbois B, Gin P, Gulmezian M, Jonassen T, Clarke CF. Complementation of *Saccharomyces cerevisiae coq7* mutants by mitochondrial targeting of the *Escherichia coli* UbiF polypeptide: two functions of yeast Coq7 polypeptide in coenzyme Q biosynthesis. *J. Biol. Chem.* 2006;281:16401-9.
15. Wang Y, Luo L, Braun OÖ et al. Neutrophil extracellular trap-microparticle complexes enhance thrombin generation via the intrinsic pathway of coagulation in mice. *Sci. Rep.* 2018;8:4020.
16. Tsui HS, Pham NVB, Amer BR et al. Human $COQ_{10}A$ and $COQ_{10}B$ are distinct lipid-binding START domain proteins required for coenzyme Q function. *J. Lipid Res.* 2019;60:1293-310.
17. Sprague GF, Jr. Assay of yeast mating reaction. *Methods Enzymol.* 1991;194:77-93.
18. Janke C, Magiera MM, Rathfelder N et al. A versatile toolbox for PCR-based tagging of yeast genes: new fluorescent proteins, more markers and promoter substitution cassettes. *Yeast* 2004;21:947-62.
19. Gietz RD, Woods RA. Transformation of yeast by lithium acetate/single-stranded carrier DNA/polyethylene glycol method. *Methods Enzymol.* 2002;350:87-96.

20. Marobbio CM, Agrimi G, Lasorsa FM, Palmieri F. Identification and functional reconstitution of yeast mitochondrial carrier for *S*-adenosylmethionine. *EMBO J.* 2003;22:5975-82.

21. Ritchie ME, Phipson B, Wu D et al. limma powers differential expression analyses for RNA-sequencing and microarray studies. *Nucleic Acids Res.* 2015;43:e47.

22. Gautier L, Cope L, Bolstad BM, Irizarry RA. affy--analysis of Affymetrix GeneChip data at the probe level. *Bioinformatics* 2004;20:307-15.

23. Glick BS, Pon LA. Isolation of highly purified mitochondria from *Saccharomyces cerevisiae. Methods Enzymol.* 1995;260:213-23.

24. Gonzalez-Hunt CP, Rooney JP, Ryde IT, Anbalagan C, Joglekar R, Meyer JN. PCR-based analysis of mitochondrial DNA copy number, mitochondrial DNA damage, and nuclear DNA damage. *Curr. Protoc. Toxicol.* 2016;67:20.11.1-20.11.25.

25. Guo X, Niemi NM, Hutchins PD et al. Ptc7p dephosphorylates select mitochondrial proteins to enhance metabolic function. *Cell Rep.* 2017;18:307-13.

26. Eyer P, Worek F, Kiderlen D et al. Molar absorption coefficients for the reduced Ellman reagent: reassessment. *Anal. Biochem.* 2003;312:224-7.

27. He CH, Xie LX, Allan CM, Tran UC, Clarke CF. Coenzyme Q supplementation or overexpression of the yeast Coq8 putative kinase stabilizes multi-subunit Coq polypeptide complexes in yeast coq null mutants. *Biochim. Biophys. Acta*. 2014;1841: 630-644

28. Schägger H, Cramer WA, von Jagow G. Analysis of molecular masses and oligomeric states of protein complexes by blue native electrophoresis and isolation of membrane protein complexes by two-dimensional native electrophoresis. *Anal. Biochem*. 1994;217: 220-230

29. Wittig, I, Braun HP, Schägger H. Blue NativePAGE. *Nat. Protoc*. 2006;1: 418-428

30. Ackerman D, Tumanov S, Qiu B et al. Triglycerides promote lipid homeostasis during hypoxic stress by balancing fatty acid saturation. *Cell Rep.* 2018;24:2596-605.

31. Wang C, Cheng D, Jalali Motlagh N et al. Highly efficient activatable MRI probe to sense myeloperoxidase activity. *J. Med. Chem.* 2021;64:5874-85.

32. Hoehn KL, Hohnen-Behrens C, Cederberg A et al. IRS1-independent defects define major nodes of insulin resistance. *Cell Metab.* 2008;7:421-33.

33. Forsman U, Sjöberg M, Turunen M, Sindelar PJ. 4-Nitrobenzoate inhibits coenzyme Q biosynthesis in mammalian cell cultures. *Nat. Chem. Biol.* 2010;6:515-7.